Superhydrophobic Surface

Superhydrophobic surfaces are proposed to be ideal blood-compatible biomaterials attributed to their beneficial characteristics.

1. Introduction

Materials with superhydrophobic properties have been receiving hefty attention since their discovery. Superhydrophobic surfaces have been vastly studied and incorporated into applications across various fields. In light of their non-wetting behavior, superhydrophobic properties have been highlighted in the development of biomaterial for medical devices. Blood-contacting medical devices are commonly seen in medical and healthcare settings, either for their diagnostic purpose or treatment purpose. Medical implants and external medical devices, including stents, vascular graft, heart valve, artificial kidney, pacemaker, guidewires, extracorporeal circulation, tubing, and catheters are examples of medical devices that are particularly close in contact with blood during their applications. Despite their inevitable role in clinical practice, blood-contacting medical devices are associated with thrombotic complications [1][2]. Furthermore, hemolysis and device-related infection are also often the major drawback of blood-contacting medical devices [3][4][5].

Many approaches have been taken in order to circumvent these problems. Nonetheless, blood compatibility remains a long-existing challenge in developing biomaterials for blood-contacting medical devices. Significant blood-compatible biomaterials suitable for medical devices are difficult to be forged as the mechanism of adhesion of blood cells and microorganisms on the surface are complex and multifactorial [6]. Boundary condition also takes part in affecting the interaction between molecules and surface. Superhydrophobic surface depicts a promising result in enhancing the blood compatibility of medical devices. The hierarchical structures on superhydrophobic surfaces have substantiated to offer good hemocompatibility by diminishing adhesion force. Blood travels across superhydrophobic surfaces with a greater velocity on the boundary layer, thus reducing the collision frequency of blood cells with the surface [7]. Consequently, this results in lesser adhesion and deformation of blood cells.

2. Characteristic of Superhydrophobic Surface

The superhydrophobic surface is defined by a surface exhibiting an apparent contact angle greater than 150°, contact angle hysteresis lesser than 10°, and sliding angle lesser than 10° [6][8]. Contact angle is the angle depicted by water droplet at the contact line when it comes in contact with the solid surface. It is commonly used as a measure of wettability. Contact angle hysteresis is the difference between the advancing contact angle and receding contact angle. It is used to evaluate the repellency of the solid surface towards the water droplet. The advancing contact angle is usually greater than the receding contact angle. The lesser the difference between these angles, the greater the non-stickiness of a droplet on the surface. In other words, superhydrophobic surface with a high apparent contact angle and low contact angle hysteresis allows the water droplet to roll off easily [9]. On the other hand, if the high apparent contact angle is accompanied by high contact angle hysteresis, this situation is known as the rose petal effect, whereby the droplet is pinned on the surface [10][11][12][13]. The differences between these two superhydrophobic wetting conditions will be further discussed in this section.

Superhydrophobicity is elucidated by two physical principles: low surface energy and high surface roughness. Both surface chemical composition and surface morphology are the major factors in interfering with the interaction between liquid and solid interface. Surface energy influences the adhesion of substances, including fluid and microorganisms, on the surface. Low surface energy reduces the work of adhesion and therefore increases the water repellency. According to Wendel's model and Cassie–Baxter's model, surface roughness plays a critical role in wettability (Figure 1). The micro/nanostructure of the surface allows entrapment of air layer beneath the contacting liquid, therefore reducing the

contact area between the liquid and solid surface [9][13][14]. Besides, the presence of air pockets on the surface endows lower frictional drag, which allows effective fluid flow [15]. Hence, the collaboration of surface roughness and low surface energy of the fluorinated polymers are to be highlighted in superhydrophobicity.
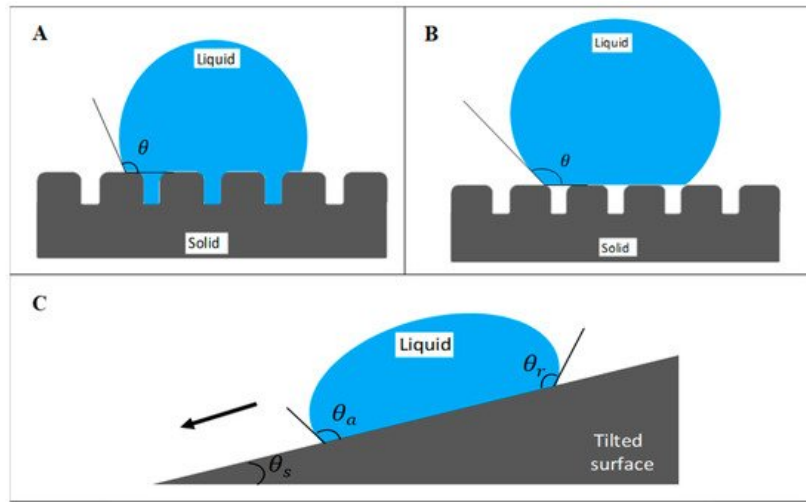

Figure 1. Wetting states of surface based on (**A**) Wenzel's model and (**B**) Cassie–Baxter's model. (**C**) Schematic of a water droplet slides off a tilted surface. θ represents the apparent contact angle, which measures the wettability of the surface by a liquid droplet. θa, θr, and θs represent advancing contact angle, receding contact angle, and sliding angle, respectively.

As the topography of the nano-/micro-scale roughened surface and/or chemically heterogeneous surface are not able to be viewed under regular optical means, hence the wetting of these surfaces is characterized by apparent contact angle [16][17]. However, pure Wenzel and Cassie–Baxter wetting states are rare to be observed in nature. Instead, a condition known as the mixed-wetting state is more common to be seen, whereby the droplet is partially supported by the air as well as the rough chemically homogenous surface [18]. It is noteworthy that the Cassie state is metastable, even on a rough surface. The entrapped air may escape and transition into the Wenzel state.

In order to maintain the thermodynamic stability of the Cassie state, the critical angle of the air entrapped below the water droplet must be small [19]. A thermodynamic equilibrium of the liquid/solid/vapor system must be attained to generate an ideal wetting surface. Air-trapping which occurs in the Cassie–Baxter state, as aforementioned, is found to be metastable as it gradually shifts to the Wenzel state [16][20][21]. Therefore, maintaining the entrapment of air pockets is important for the Cassie regime as the irreversible transition can be due to the invasion, such as condensation or evaporation of water droplets, or through external pressure [21]. The superhydrophobic surface loses its water-repellent properties when the air gap between the structured surface is filled with water. The Cassie–Baxter state demonstrated weak drop adhesion and reduced friction properties, therefore providing the "Lotus effect" or self-cleaning properties. Remarkably, shifting from the Cassie–Baxter state to the Wenzel state affects the drag reduction by altering the flow rate [15]. Besides, the surface loses its self-cleaning effect and promotes adhesion of the water droplets instead when the wetting state shifts from the Cassie–Baxter to the Wenzel regime [21][22]. The Wenzel state allows the water droplet to pin on the surface (known as the rose petal effect) while exhibiting higher contact angle hysteresis, as compared to the Cassie state, which exhibits low contact angle hysteresis [20]. The Wenzel state promotes the pinning of the droplet on the surface due to the complete wetting on the ground level of texture [21][22]. Based on the distinction between both wetting states, the Cassie–Baxter regime is hence preferable and should be taken into consideration during the development and fabrication of superhydrophobic surfaces in medical devices.

3. Development of Superhydrophobic Surface

The principles of superhydrophobic surface are inspired by nature (Table 1). The most classic example would be the lotus leaf. Besides having a high contact angle, the hierarchical structure on the lotus leaf endows its superhydrophobicity. The term "Lotus effect" is derived from its self-cleaning behavior. Non-adhesive lotus leaf surface is able to repel water droplets and allows them to easily slide off. Further examples of superhydrophobic surfaces that can be found in nature are available in other studies [23][24]. While producing superhydrophobic surfaces by mimicking lotus leaf is the most common approach among previous studies, endothelial cells lining of a human blood vessel is also another biomimetic structural superhydrophobic surface [25].

Table 1. Examples of superhydrophobic surfaces present in nature.

	Contact Angle (°)	References
Plant		
Lotus leaf (*Nelumbo nucifera*)	**162**	[24]
Rice leaf (*Oryza sativa*)	**157**	[26]
Chinese watermelon	**159**	[26]
Lyme grass (*Leymus arenarius*)	**161**	[27]
Perfoliate knotweed (*Polygonum perroliatum*)	**162**	[26]
Ramee leaf (*Boehmeria nivea*)	**164**	[26]
Taro plant leaf (*Colocasia esculenta*)	**164**	[27]
Purple setcreasea (*Setcreasea purpurea*)	**167**	[26]
Insect		
Horsefly (*Tabanus chrysurus*) wings	**156**	[26]
Butterfly (*Parantica sita*) wings	**161**	[28]
Walker's cicada (*Meimuna opalifera) wings*	**165**	[26]
Water strider legs	**167.6**	[29]

Artificial superhydrophobic surfaces can be produced via different routes and techniques, including surface treatment, changing their surface composition, or altering their surface texture (Table 2). Some materials hitherto less hydrophobic can be transformed into superhydrophobic via modifications. For example, hydrophilic polyvinyl alcohol (PVA) film (contact angle 72.1°) was transformed into a superhydrophobic film (contact angle 171.2°) by adding PVA nanofibers [30]. The addition of silicon nanofibers increases the contact angle of a hydrogen-terminated silicon surface from 74° to 160° [31]. Introduction of nanostructures and fluorinated alkyl side chains on smooth poly(carbonate urethane) film increases its contact angle from 109.1° to 163.6° [32]. The progress of developing an efficient superhydrophobic surface during the past few years has been reviewed. Different types of approaches to fabricate superhydrophobic surfaces have been analyzed [9][13][33][34].

Table 2. Examples of artificial superhydrophobic surfaces.

Materials	Fabrication Process	Contact Angle (°)	References
Carbon nanofiber coating	**Mixing of carbon nanofiber with polytetrafluoroethylene to form composite dispersion**	**162.1**	[35]
Fluorinated polymer foam (Fluoropor)	**Photoinitiated radical polymerization of fluorinated perfluoropolyether methacrylate and alcohol derivatives**	**163.7**	[36]
Graphene	**Reduced graphene oxide surface-treated with silane**	**157**	[37]
Polystyrene film	**Vacuum casting of polystyrene film on porous template**	**151**	[38]
	Electrospinning of polystyrene film and modified with perfluorodecyltrichlorosilane vapor deposition	**168**	[39]
Polytetrafluoroethylene	**Plasma etching treatment using argon and oxygen gases**	**171.4**	[40]
Silicon dioxide	**Mixing of silicon dioxide nanoparticles with poly(methyl methacrylate) to form a dispersion**	**163.3**	[41]
Titanium	**Adonization process and modified with chemical vapor deposition of (heptadecafluoro-1,1,2,2-tetrahydrodecyl)trichlorosilane**	**164**	[42]

As aforementioned, surface morphology can act as a significant factor in influencing superhydrophobicity. Surface roughness endows a higher apparent contact angle, therefore enhancing the wettability of the surface. As described by Cassie and Baxter, the surface texture creates air pockets between the protrusions. These air pockets limit the contact point between the liquid and solid surface. Modifying surface texture is a simple and economical way to enhance superhydrophobic properties. With the help of modern technology, surface roughness can be increased, for instance,

through oxygen plasma treatment or via a simple lithography technique known as the nanoimprint process to create nanostructures on the surfaces [43]. On the other hand, modification of the surface chemical composition is another alternative to prepare a superhydrophobic surface [44].

The height of protrusion that made up the hierarchical patterned surface acts as a factor in swaying the self-cleaning ability of the surface. As the protrusion is sufficiently high to allow the contaminant partially to fill in between them, or the contaminant is small enough to penetrate the coating, it will produce a surface with increased roll-off angle, whereby the self-cleaning effect is futile. Micro/nanopatterned surfaces with pore sizes below 500 nm withstand most kinds of particulate contamination [45]. On the other hand, another study indicated that microstructured surfaces with protrusions size range below 5 μm can be cleaned easily by fog, as the size of water droplets within the fog appears to be higher than that [46].

Self-cleaning can be enhanced by introducing structures with appropriate height and width on the surface. Low protrusion height and wide protrusion size endow a larger contact area for the contaminant to attach, which causes higher difficulty in removal. As the distance between the protrusion is sufficient to disable the filling of the contaminant in between, and at the same time, the water droplets elevated by the protrusions confer a low roll-off angle, the self-cleaning effect is said to be plausible [46].

Superhydrophobic properties can be enhanced by altering the surface structure while maintaining the chemical composition of the target surface, as reported by Mao et al. and Ryu et al. [38][40]. Both studies transformed smooth polymer surfaces into an ideal blood-contacting superhydrophobic biomaterial. Mao et al. fabricated polystyrene nanotube films by mimicking the structure of lotus leaf, whereas Ryu et al. performed plasma-etching on polytetrafluoroethylene. The superhydrophobic polymer surfaces exhibit high contact angles, 151° and 171.4°, respectively. In addition to their self-cleaning effect, the surface also demonstrated high durability, although negligible deformation on the nanoscale structure surface was observed under SEM after prolonged usage and exposure to air. Importantly, the nano/microstructures of superhydrophobic films contribute to the low adhesion of blood cells and platelets. On the other hand, Helmer et al. fabricated a transparent fluorinated polymer foam via a simple one-step photoinitiated radical polymerization [36]. The nano/microstructure of the foam-like polymer provides its superhydrophobic characteristic with a contact angle of 163.7° and a contact angle hysteresis of 6.1°. This easy-to-fabricate material is resistant to abrasion as well. The hierarchical surface roughness is substantiated to increase the superhydrophobic effect, thus improving the anticoagulation and blood-repellent effects.

References

1. Jaffer, I.H.; Weitz, J.I. Acta Biomaterialia The blood compatibility challenge. Part 1: Blood-contacting medical devices: The scope of the problem. Acta Biomater. 2019, 94, 2–10.

2. Ratner, B.D. The catastrophe revisited: Blood compatibility in the 21st Century. Biomaterials 2007, 28, 5144–5147.

3. Bark, D.L., Jr.; Vahabi, H.; Bui, H.; Movafaghi, S.; Moore, B.; Kota, A.K.; Popat, K.; Dasi, L.P. Hemodynamic Performance and Thrombogenic Properties of a Superhydrophobic Bileaflet Mechanical Heart Valve. Ann. Biomed. Eng. 2017, 45, 452–463.

4. Falde, E.J.; Yohe, S.T.; Colson, Y.L.; Grinstaff, M.W. Superhydrophobic materials for biomedical applications. Biomaterials 2016, 104, 87–103.

5. Yasuda, T.; Shimokasa, K.; Funakubo, A.; Higami, T.; Kawamura, T.; Fukui, Y. An Investigation of Blood Flow Behavior and Hemolysis in Artificial Organs. ASAIO J. 2000, 46, 527–531.

6. Hoshian, S.; Kankuri, E.; Ras, R.H.A.; Franssila, S.; Jokinen, V. Water and Blood Repellent Flexible Tubes. Sci. Rep. 2017, 7, 16019.

7. Fan, H.; Chen, P.; Qi, R.; Zhai, J.; Wang, J.; Chen, L.; Chen, L.; Sun, Q.; Song, Y.; Han, D.; et al. Greatly Improved Blood Compatibility by Microscopic Multiscale Design of Surface Architectures. Small 2009, 5, 2144–2148.

8. Butt, H.-J.; Roisman, I.V.; Brinkmann, M.; Papadopoulos, P.; Vollmer, D.; Semprebon, C. Characterization of super liquid-repellent surfaces. Curr. Opin. Colloid Interface Sci. 2014, 19, 343–354.

9. Roach, P.; Shirtcliffe, N.J.; Newton, M.I. Progess in superhydrophobic surface development. Soft Matter 2008, 4, 224–240.

10. Bhushan, B.; Nosonovsky, M. The rose petal effect and the modes of superhydrophobicity. Philos. Trans. R. Soc. A Math. Phys. Eng. Sci. 2010, 368, 4713–4728.

11. Feng, L.; Zhang, Y.; Xi, J.; Zhu, Y.; Wang, N.; Xia, F.; Jiang, L. Petal Effect: A Superhydrophobic State with High Adhesive Force. Langmuir 2008, 24, 4114–4119.

12. Park, Y.M.; Gang, M.; Seo, Y.H.; Kim, B.H. Artificial petal surface based on hierarchical micro- and nanostructures. Thin Solid Films 2011, 520, 362–367.

13. Jeevahan, J.; Chandrasekaran, M.; Britto Joseph, G.; Durairaj, R.B.; Mageshwaran, G. Superhydrophobic surfaces: A review on fundamentals, applications, and challenges. J. Coat. Technol. Res. 2018, 15, 231–250.

14. Verplanck, N.; Galopin, E.; Camart, J.-C.; Thomy, V.; Coffinier, Y.; Boukherroub, R. Reversible Electrowetting on Superhydrophobic Silicon Nanowires. Nano Lett. 2007, 7, 813–817.

15. McHale, G.; Newton, M.I.; Shirtcliffe, N.J. Immersed superhydrophobic surfaces: Gas exchange, slip and drag reduction properties. Soft Matter 2010, 6, 714–719.

16. Bormashenko, E.Y. Physics of Wetting: Phenomena and Applications of Fluids on Surfaces; De Gruyter: Berlin, Germany; ISBN 978-3-11-044481-0.

17. Marmur, A. A guide to the equilibrium contact angles maze. Contact Angle Wettability Adhes. 2009, 6, 3–18.

18. Miwa, M.; Nakajima, A.; Fujishima, A.; Hashimoto, K.; Watanabe, T. Effects of the Surface Roughness on Sliding Angles of Water Droplets on Superhydrophobic Surfaces. Langmuir 2000, 16, 5754–5760.

19. Scarratt, L.R.J.; Steiner, U.; Neto, C. A review on the mechanical and thermodynamic robustness of superhydrophobic surfaces. Adv. Colloid Interface Sci. 2017, 246, 133–152.

20. Bormashenko, E.Y. Wetting of Real Surfaces; De Gruyter, Inc.: Berlin, Germany, 2013; ISBN 9783110258790.

21. Lafuma, A.; Quéré, D. Superhydrophobic states. Nat. Mater. 2003, 2, 457–460.

22. Vinogradova, O.I.; Dubov, A.L. Superhydrophobic Textures for Microfluidics. Mendeleev Commun. 2012, 22, 229–236.

23. Darmanin, T.; Guittard, F. Superhydrophobic and superoleophobic properties in nature. Mater. Today 2015, 18, 273–285.

24. Neinhuis, C.; Barthlott, W. Characterization and Distribution of Water-repellent, Self-cleaning Plant Surfaces. Ann. Bot. 1997, 79, 667–677.

25. Chen, L.; Han, D.; Jiang, L. On improving blood compatibility: From bioinspired to synthetic design and fabrication of biointerfacial topography at micro/nano scales. Colloids Surf. B Biointerfaces 2011, 85, 2–7.

26. Wolfs, M.; Darmanin, T.; Guittard, F. Superhydrophobic Fibrous Polymers. Polym. Rev. 2013, 53, 460–505.

27. Koch, K.; Barthlott, W. Superhydrophobic and superhydrophilic plant surfaces: An inspiration for biomimetic materials. Philos. Trans. R. Soc. A Math. Phys. Eng. Sci. 2009, 367, 1487–1509.

28. Perez Goodwyn, P.; Maezono, Y.; Hosoda, N.; Fujisaki, K. Waterproof and translucent wings at the same time: Problems and solutions in butterflies. Naturwissenschaften 2009, 96, 781–787.

29. Gao, X.; Jiang, L. Water-repellent legs of water striders. Nature 2004, 432, 36.

30. Feng, L.; Li, S.; Li, Y.; Li, H.; Zhang, L.; Zhai, J.; Song, Y.; Liu, B.; Jiang, L.; Zhu, D. Super-Hydrophobic Surfaces: From Natural to Artificial. Adv. Mater. 2002, 14, 1857–1860.

31. Cao, L.; Hu, H.-H.; Gao, D. Design and Fabrication of Micro-textures for Inducing a Superhydrophobic Behavior on Hydrophilic Materials. Langmuir 2007, 23, 4310–4314.

32. Sun, T.; Tan, H.; Han, D.; Fu, Q.; Jiang, L. No Platelet Can Adhere—Largely Improved Blood Compatibility on Nanostructured Superhydrophobic Surfaces. Small 2005, 1, 959–963.

33. Lim, J.I.; Kim, S.I.; Jung, Y.; Kim, S.H. Fabrication and medical applications of lotus-leaf-like structured superhydrophobic surfaces. Polymer 2013, 37, 411–419.

34. Avrămescu, R.-E.; Ghica, M.V.; Dinu-Pîrvu, C.; Prisada, R.; Popa, L. Superhydrophobic Natural and Artificial Surfaces-A Structural Approach. Mater 2018, 11, 866.

35. Li, Z.; Milionis, A.; Zheng, Y.; Yee, M.; Codispoti, L.; Tan, F.; Poulikakos, D.; Yap, C.H. Superhydrophobic hemostatic nanofiber composites for fast clotting and minimal adhesion. Nat. Commun. 2019, 10, 5562.

36. Helmer, D.; Keller, N.; Kotz, F.; Stolz, F.; Greiner, C.; Nargang, T.M.; Sachsenheimer, K.; Rapp, B.E. Transparent, abrasion-insensitive superhydrophobic coatings for real-world applications. Sci. Rep. 2017, 7, 15078.

37. Lee, J.-S.; Yoon, J.-C.; Jang, J.-H. A route towards superhydrophobic graphene surfaces: Surface-treated reduced graphene oxide spheres. J. Mater. Chem. A 2013, 1, 7312–7315.

38. Mao, C.; Zhao, W.-B.; Luo, W.-P.; Liang, C.-X.; Hou, X.-M.; Huang, X.-H.; Liu, H.-K.; Xiao, Y.-H.; Bao, J.-C.; Shen, J. Geometric bionics: Lotus effect helps polystyrene nanotube films get good blood compatibility. Nat. Preced. 2009.

39. Yuan, Y.; Hays, M.P.; Hardwidge, P.R.; Kim, J. Surface characteristics influencing bacterial adhesion to polymeric substrates. RSC Adv. 2017, 7, 14254–14261.

40. Ryu, J.; Kim, K.; Park, J.; Hwang, B.G.; Ko, Y.; Kim, H.; Han, J.; Seo, E.; Park, Y.; Lee, S.J. Nearly Perfect Durable Superhydrophobic Surfaces Fabricated by a Simple One-Step Plasma Treatment. Sci. Rep. 2017, 7, 1981.

41. Wang, J.; Chen, X.; Kang, Y.; Yang, G.; Yu, L.; Zhang, P. Preparation of superhydrophobic poly(methyl methacrylate)-silicon dioxide nanocomposite films. Appl. Surf. Sci. 2010, 257, 1473–1477.

42. Bartlet, K.; Movafaghi, S.; Dasi, L.P.; Kota, A.K.; Popat, K.C. Antibacterial activity on superhydrophobic titania nanotube arrays. Colloids Surf. B Biointerfaces 2018, 166, 179–186.

43. Shiu, J.-Y.; Whang, W.-T.; Chen, P. Superhydrophobic Coatings for Microdevices. J. Adhes. Sci. Technol. 2008, 22, 1883–1891.

44. Wu, Y.; Wang, J.; Zhang, D.; Li, L.; Zhu, Y. Preparation and characterization of superhydrophobic surface based on polydimethylsiloxane (PDMS). J. Adhes. Sci. Technol. 2019, 33, 1870–1881.

45. Geyer, F.; D'Acunzi, M.; Sharifi-Aghili, A.; Saal, A.; Gao, N.; Kaltbeitzel, A.; Sloot, T.-F.; Berger, R.; Butt, H.-J.; Vollmer, D. When and how self-cleaning of superhydrophobic surfaces works. Sci. Adv. 2020, 6, eaaw9727.

46. Fürstner, R.; Barthlott, W.; Neinhuis, C.; Walzel, P. Wetting and Self-Cleaning Properties of Artificial Superhydrophobic Surfaces. Langmuir 2005, 21, 956–961.